Molecular Biology of the Cell
Vol. 11, 4259–4275, December 2000

Exocyst Is Involved in Cystogenesis and Tubulogenesis and Acts by Modulating Synthesis and Delivery of Basolateral Plasma Membrane and Secretory Proteins

Joshua H. Lipschutz,* Wei Guo,† Lucy E. O'Brien,‡ Yen H. Nguyen,‡ Peter Novick,† and Keith E. Mostov‡§

*Departments of Anatomy and Medicine, University of California, San Francisco, San Francisco, California 94143-0452; †Department of Cell Biology, Yale University School of Medicine, New Haven, Connecticut 06520-8002; and ‡Departments of Anatomy, Biochemistry, and Biophysics, and the Cardiovascular Research Institute, University of California, San Francisco, San Francisco, California 94143-0452

Submitted June 15, 2000; Revised August 25, 2000; Accepted September 28, 2000
Monitoring Editor: Suzanne R. Pfeffer

Epithelial cyst and tubule formation are critical processes that involve transient, highly choreographed changes in cell polarity. Factors controlling these changes in polarity are largely unknown. One candidate factor is the highly conserved eight-member protein complex called the exocyst. We show that during tubulogenesis in an in vitro model system the exocyst relocalized along growing tubules consistent with changes in cell polarity. In yeast, the exocyst subunit Sec10p is a crucial component linking polarized exocytic vesicles with the rest of the exocyst complex and, ultimately, the plasma membrane. When the exocyst subunit human Sec10 was exogenously expressed in epithelial Madin-Darby canine kidney cells, there was a selective increase in the synthesis and delivery of apical and basolateral secretory proteins and a basolateral plasma membrane protein, but not an apical plasma membrane protein. Overexpression of human Sec10 resulted in more efficient and rapid cyst formation and increased tubule formation upon stimulation with hepatocyte growth factor. We conclude that the exocyst plays a central role in the development of epithelial cysts and tubules.

INTRODUCTION

Epithelial organs consist mainly of spherical and tubular structures. Formation of these cysts and tubules represents complex, poorly understood processes involving multiple factors and receptors that are crucial for the development of many mammalian organs, including the kidney, lung, mammary gland, salivary gland, and pancreas (Gumbiner, 1992; Sakurai *et al.*, 1997a,b; Vainio and Muller, 1997; Pollack *et al.*, 1998). Cystogenesis and tubulogenesis are also centrally involved in such diverse processes as organ regeneration after injury and autosomal dominant polycystic kidney disease (ADPKD) (Grantham, 1997; Balkovetz and Lipschutz, 1998).

A significant advance for the study of cystogenesis and tubulogenesis was the development of an in vitro model system using collagen gel cultures of Madin-Darby canine kidney (MDCK) epithelial cells stimulated by hepatocyte growth factor (HGF) (Montesano *et al.*, 1991a,b). HGF has been shown to induce epithelial cell morphogenesis into organ-like structures that are characteristic of the organ from which the cells were originally derived (Brinkmann *et al.*, 1995). MDCK cells are derived from canine renal tubular epithelium (Simons and Fuller, 1985) and form hollow fluid-filled cysts when cultured in collagen. Exposure of these preformed cysts to HGF causes the cysts to develop branching tubules in a process that resembles renal tubulogenesis in vivo (Saxen, 1987; Lipschutz, 1998). Multiple investigators have used this in vitro system to study various aspects of tubulogenesis (Santos *et al.*, 1993; Santos and Nigam, 1993; Cantley *et al.*, 1994; Barros *et al.*, 1995; Derman *et al.*, 1995; Weidner *et al.*, 1995; Crepaldi *et al.*, 1997; Boccaccio *et al.*, 1998).

HGF is also known as scatter factor, based on its ability to cause MDCK cells to scatter (Stoker and Perryman, 1985; Stoker *et al.*, 1987; Gherardi *et al.*, 1989). This scattering

§ Corresponding author. E-mail address: mostov@itsa.ucsf.edu.
Abbreviations used: ADPKD, autosomal dominant polycystic kidney disease; HGF, hepatocyte growth factor; hSec10, human Sec10; MDCK, Madin-Darby canine kidney.

activity originally led to the proposal of a two-step dissociation/reassociation model of tubulogenesis in which MDCK cells detach from the cyst, lose polarity, and migrate out as single cells into the collagen matrix. The migrating single cells were then proposed to coalesce and reassemble into multicellular structures that form tubules of polarized cells (Thiery and Boyer, 1992). However, we recently showed that this model was incorrect and that cells in the cyst, when exposed to HGF, initially sent out long extensions of their basolateral surface. Cells then migrated out to form short chains of cells that lacked apico-basolateral polarity and were surrounded by basolateral surface (Pollack *et al.*, 1998). During this process, cell–cell contacts were differentially regulated. E-cadherin was randomly distributed around the cell surface, desmoplakins I/II accumulated intracellularly, and the tight junction protein ZO-1 remained localized at sites of cell–cell contact. Further migration and division led to cords of cells, with nascent lumina appearing between the cells as they began to repolarize, eventually forming mature tubules (Pollack *et al.*, 1998). Our results indicated that transient loss and restoration of cell polarity was a crucial component of tubulogenesis. Factors regulating this physiological modulation of polarity during tubule formation are not known. One candidate factor is the eight-subunit exocyst complex, six of whose member proteins were discovered through studies of polarized secretion in yeast (Novick *et al.*, 1980).

The budding yeast *Saccharomyces cerevisiae* represents a simple model organism in which to study polarized secretion and exocytosis. Exocytosis in yeast occurs at distinct plasma membrane subdomains, which vary with the cell cycle. Unbudded cells polarize secretion to the new bud site before bud emergence and continue to direct secretion to the tip of the emerging bud (Tkacz and Lampen, 1972; Farkas *et al.*, 1974; Field and Schekman, 1980). When the daughter cell is about two-thirds the size of the mother cell, secretion becomes isotropic over the surface of the daughter cell, whereas very little growth or secretion occurs in the mother cell. After nuclear division, the secretory pathway orients to the mother-bud neck, resulting in cytokinesis and septation (Byers, 1981). The exocyst is a determinant of polarized secretion throughout the yeast life cycle and Sec3p, a subunit of the exocyst, likely represents the spatial landmark that defines the sites of exocytosis (Novick *et al.*, 1980; Finger *et al.*, 1998). The exocyst is a 750-kDa complex comprised of Sec3p, Sec5p, Sec6p, Sec8p, Sec10p, Sec15p, Exo70p, and Exo84p (Terbush *et al.*, 1996; Guo *et al.*, 1999a). In yeast, Sec10p and Sec15p exist as a subcomplex that acts as a bridge between the rab GTPase Sec4p on the vesicle and the rest of the exocyst and, ultimately, the plasma membrane (Guo *et al.*, 1999b). Furthermore, in yeast overexpression of the carboxy terminal domain of Sec10p resulted in an enlarged elongated bud, whereas overexpression of the amino terminal two-thirds of Sec10p inhibited exocytosis (Roth *et al.*, 1998). Overexpression of full-length sec10 in yeast had no discernible effect, though that may be due to the fact that sec10 overexpression with the GAL promoter did not reach a phenotypic threshold level (Guo and Novick, unpublished observations).

In yeast, the exocyst acts by targeting secretory vesicles to the sites of exocytosis. In mammalian epithelial cells the tight junction acts as a physical barrier between the apical and basolateral plasma membranes (Yeaman *et al.*, 1999). It was hypothesized as early as 1980 that polarized vesicles containing proteins destined for the plasma membranes are first targeted to the area around the tight junction (Louvard, 1980). In fully polarized epithelial cells, the mammalian exocyst (also called the Sec6/8 complex) localized to the tight junction, suggesting a role in membrane traffic (Grindstaff *et al.*, 1998). Highly conserved mammalian homologues of all eight yeast proteins have been identified (Hsu *et al.*, 1998). In isolated nonpolarized MDCK cells the exocyst was largely intracellular, in early contact cells the exocyst localized to the area of cell–cell contact, and, as polarity became established, the exocyst relocalized to the tight junction. In streptolysin-O-permeabilized MDCK cells, antibodies to Sec8p inhibited delivery of a basolateral plasma membrane protein, the exogenously expressed low-density lipoprotein receptor, from the trans-Golgi network to the basolateral surface but did not affect the delivery of an exogenously expressed apical plasma membrane protein, $p75^{NTR}$, demonstrating a role for the mammalian exocyst in polarized membrane traffic (Grindstaff *et al.*, 1998). Here we have investigated the role of the exocyst in epithelial cyst and tubule formation.

MATERIALS AND METHODS

Cystogenesis and Tubulogenesis

MDCK type II cells were maintained in minimum essential medium (MEM) supplemented with 5% fetal calf serum. For growth of cells in collagen gels, MDCK cells were trypsinized and triturated into a single-cell suspension of 2×10^4 cells/ml in a type I collagen solution as described previously (Pollack *et al.*, 1998). Cells in suspension were plated onto 10-mm filters (0.02–0.2-μm pore size; Nunc, Naperville, IL) and the collagen was allowed to gel before addition of medium. Medium was changed every 4 d. After 10 d, conditioned medium containing HGF from MRC5 human lung fibroblasts (ATCC CCL171) was added to the cultures.

Immunofluorescence, Confocal, and Electron Microscopy (EM)

Cells in collagen gel were rinsed in phosphate-buffered saline and fixed for 30 min with 4% paraformaldehyde after digesting in collagenase (100 U/ml; Sigma, St. Louis, MO) for 10 min at 37°C as previously described (Pollack *et al.*, 1998). Nonspecific binding sites were blocked and the cells permeabilized by using 0.7% fish skin gelatin and 0.025% saponin. Samples were placed in medium containing primary antibody at the following concentrations: Sec6 1:100 (StressGen, Victoria, Canada), rSec8 1:100 (StressGen), Alexa 488 and 594 phalloidin 1:50 (Molecular Probes, Eugene, OR), human Sec10 (hSec10) (1:100) (Guo *et al.*, 1997). After extensive washing, the samples were incubated in blocking buffer containing Alexa 488 or 594-conjugated secondary antibody, 1:200 dilution (Molecular Probes). Cells were postfixed with 4% paraformaldehyde and mounted. Confocal images were collected by using a krypton-argon laser (Bio-Rad 1024). For EM, filter-grown cells were fixed in a solution containing 2% glutaraldehyde, 0.8% paraformaldehyde, and 0.1 M cacodylate. The cells were stained with osmium and imidazole as previously described (Thiery *et al.*, 1995), dehydrated, embedded in resin, sectioned, and imaged (Zeiss 10CA). For endocytic labeling of vesicles, filter-grown cells were exposed to apical and basolateral media containing 1 mg/ml horseradish peroxidase (Sigma) for 10 min. Cells were then lightly fixed (in a solution containing 1.5% glutaraldehyde, 0.1 M cacodylate, and 1% sucrose), washed with buffer (0.1 M cacodylate, 3% sucrose), incubated with

peroxidase substrate (10 ml of 0.05 M Tris, pH 7.6, 5 mg of diamino benzidine, 5% sucrose) followed by 1% H_2O_2, dehydrated, embedded in resin, and sectioned as described above.

Transfection

hSec10 was subcloned and placed into PCDNA3 (Invitrogen, San Diego, CA) after addition of a C-terminal myc epitope tag. The plasmid was transfected into MDCK type II cells by using the calcium-phosphate precipitation method (Sambrook *et al.*, 1989; Breitfeld *et al.*, 1989). Clones were selected by resistance to G418 and were kept under selection for subsequent experiments. The control (empty plasmid transfected) cells were a pooled line (i.e. nonclonal) to avoid clonal variation. Similar results were obtained with individual clonal control lines (Lipschutz and Mostov, unpublished observations). Clones expressing hSec10p-myc were identified by Western blot with 9E10 anti-myc antibody (Santa Cruz Biotechnology, Santa Cruz, CA) at 1:1000 dilution, goat anti-mouse HRP (Jackson ImmunoResearch, West Grove, PA) as the secondary antibody, and enhanced chemiluminescence (ECL) (NEN, Boston, MA). Equal amounts of total protein were assayed as determined by the bicinchoninic protein assay (Pierce, Rockford, IL), Ponceau Red staining, and Western blotting with antibody (1:1000) against cytosolic proteins p42 and p44 MAP Kinase (New England Biolabs, Beverly, MA).

Western Blot and Immunoprecipitation

Cells were lysed in 0.5% SDS lysis buffer (0.5% SDS, 100 mM NaCl, 50 mM tetraethylammonium-Cl, pH 8.1, 5 mM EDTA, 0.2% Trasylol, and 0.02% NaN_3) and prepared in standard manner (Breitfeld *et al.*, 1989). For immunoprecipitation, 4 μl of protein A-sepharose beads coupled to 8 μg of anti-rSec8 antibody (StressGen) or 12 μg of 9E10 antibody (anti-myc) conjugated to agarose (Santa Cruz Biotechnology) were incubated overnight with the cell lysate (after addition of equal volumes of 2.5% Triton X-100 in 100 mM tetraethylammonium buffer, pH 8). The immunoprecipitated proteins were eluted and separated by SDS-PAGE and the proteins transferred onto nitrocellulose. The protein bands were detected by incubations with the appropriate primary antibody, followed by goat anti-mouse HRP (Jackson ImmunoResearch) as the secondary antibody, and ECL (NEN). Quantification of bands was performed on scanned images by using the IPlab Gel program (Signal Analytics).

Quantitation of Association of Sec8p and hSec10p by Coimmunoprecipitation

hSec10 overexpressing cells grown to confluency on a 10-cm dish were lysed in 1 ml of NP-40 lysis buffer (Calbiochem, La Jolla, CA) (1% NP-40, 125 mM NaCl, and 20 mM HEPES, pH 7.4). Four sequential rounds of immunoprecipitation were performed using antibody against Sec8p (14G1; Stressgen). Anti-Sec8 (8 μg) antibody and 4 μl of protein A-sepharose beads were added. After incubation at 4°C for 4–12 h the beads were pelleted by low-speed centrifugation and the supernatant was transferred to a new tube. The beads were washed five times in NP-40 lysis buffer. The next round of immunoprecipitation was performed on the supernatant, by adding the same amount of anti-Sec8 antibody and beads, and repeating the incubation. After the fourth round of immunoprecipitation with antibody to Sec8p, a fifth and final round was performed with 9E10 antibody to the myc epitope tag. The 9E10 immunoprecipitation was performed by adding 12 μg of 9E10 antibody (anti-myc) conjugated to agarose (Santa Cruz Biotechnology) and incubating for 12 h at 4°C. The washed beads from all five immunoprecipitates were analyzed by SDS-PAGE, blotted, and the blot probed with both antibody to Sec8p and antibody to myc and visualized with goat anti-mouse HRP (as the secondary antibody) and ECL. Intensities of all bands were quantitated by using the IPlab Gel program (Signal Analytics, Vienna, VA). The total amount of Sec8p immunoprecipitated in all five immunoprecipitates was taken as 100%, and of this 81% was found in the sum of rounds 1 to 4. Therefore, the first four rounds were sufficient to immunoprecipitate the vast majority of Sec8p. We then asked what percentage of the hSec10p was associated with the Sec8p immunoprecipitated during the first four rounds. The total hSec10p was taken as the sum of the hSec10 bands in all five rounds of immunoprecipitation. The fraction of hSec10p that associates with Sec8p was taken as the sum of hSec10p that coimmunoprecipitated with the Sec8p in the first four rounds of immunoprecipitation with anti-Sec8p antibody, divided by the total hSec10p. Note that a minority (35%) of hSec10p coimmunoprecipitated with the Sec8p in the first four rounds, and most hSec10p (65%) only immunoprecipitated with the antibody to its myc tag in the fifth round.

To perform the reciprocal experiment, that is, to determine what fraction of Sec8p could be coimmunoprecipitated with hSec10p, we first immunoprecipitated a duplicate cell lysate with four rounds of antibody to the myc tag on the hSec10. A fifth and final round was then performed by using antibody to Sec8p (all immunoprecipitation conditions were as described above except 12 μg of anti-Sec8 antibody, an amount sufficient to immunoprecipitate all the endogenous canine Sec8 in a 10-cm plate of confluent cells, was used). The first four rounds were sufficient to immunoprecipitate 86% of the hSec10p. We then determined the fraction of Sec8p that was immunoprecipitated with the hSec10p. The total Sec8p was taken as the sum of all five rounds. The fraction of Sec8p that associates with hSec10p was taken as the sum of Sec8p in rounds 1 to 4, divided by the total Sec8p. Note unlike the experiment described above, the majority of endogenous canine Sec8p (65%) coimmunoprecipitated with the hSec10p in the first four rounds, and only 35% was immunoprecipitated with the antibody to Sec8p in the fifth round.

Synthesis, Secretion, and Surface Delivery Assays

Cells from a confluent 10-cm plastic dish were trypsinized and 5% of the cells were seeded per 12-mm (0.4-μm pore size) filter (Costar, Cambridge, MA). The cells were grown for 5–6 d with fresh medium added daily. The cells were washed with phosphate-buffered saline and starved for 15 min in MEM lacking methionine. Cells were then labeled by exposing the basolateral surface to a 25-μl drop of starvation medium containing 4 μl of [^{35}S]methionine (31.4 μCi/ul; NEN) for 20 min. For synthesis assays, after pulsing with [^{35}S]methionine for 20 min, cells were lysed in 0.5% SDS, equal volumes of 2.5% Triton X-100 were added, and immunoprecipitation was performed by using antibody against gp80 (a kind gift from D. Sabatini, New York University, NY), E-Cadherin (a kind gift from W.J. Nelson, Stanford, CA), or gp135 (a generous gift from G. Ojakian, State University of New York, NY).

For secretion assays, the cells were labeled as described above, washed extensively, and MEM was added (0.3 ml apically and 0.5 ml basolaterally) and collected at the time points noted. The filters were grown in triplicate for each experiment, and each experiment was repeated at least three times.

Surface delivery assays of E-Cadherin and gp135 were performed as described above except cells were pulsed with [^{35}S]methionine for 20 min, washed extensively, allowed to chase for 60 min, and Sulfo-NHS-Biotin (EZ-Link; Pierce) was added at 0.5 mg/ml. Immunoprecipitation with antibody against E-Cadherin and gp135 was performed. The antibody–beads–antigen complex was then boiled and the supernatant was reprecipitated with streptavidin beads and the remaining proteins run on an SDS-PAGE gel and analyzed with a phosphorimager (Molecular Dynamics). Modified from Le Bivic *et al.* (1990).

Transcytosis Assay

Cells expressed transfected rabbit polymeric immunoglobulin receptor. Briefly, cells were cultured as described above and exposed

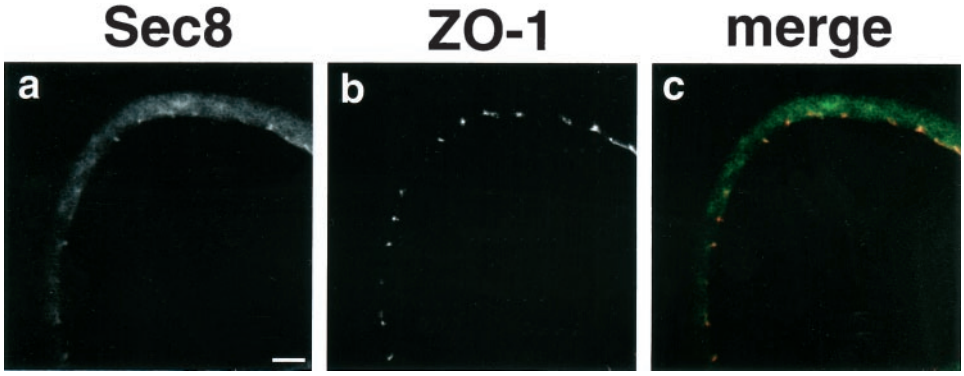

Figure 1. Sec8p partially localizes at the tight junction in cysts. This figure is a confocal section through the middle of a mature, fully polarized cyst formed by MDCK cells grown for 10 d in a collagen matrix. Antibody against Sec8p (a) and antibody against the tight junction protein ZO-1 (b) show colocalization as demonstrated by the yellow color in the merged panel (c). Sec 8, green; ZO-1, red. Bar, 10 μm.

at the basolateral surface to a 25-μl drop of medium containing 4 μl of ^{125}I-IgA. The ^{125}I-IgA was allowed to internalize for 10 min and fresh medium was added apically and basolaterally. The medium was collected at various time points and the fractions were quantified in a gamma-counter as previously described (Luton *et al.*, 1998). The filters were grown in triplicate for each assay, and each assay was repeated three times.

Glycerol Gradient

Contact-naive control and MDCK cells overexpressing hSec10 were homogenized in a sucrose buffer [20 mM HEPES-KOH, pH 8, 90 mM KOAc, 2 mM Mg(OAc)2, and 250 mM sucrose] by repeated passage through a 27-gauge needle. The postnuclear supernatant was centrifuged at 15,000 $\times$ *g* for 10 min. The resulting supernatant was fractionated in a linear 22.5–36% (wt/wt) glycerol gradient by centrifugation at 80,000 $\times$ *g* for 16 h as previously described (Ting *et al.*, 1995; Grindstaff *et al.*, 1998). Fractions (110 μl) from 1.2 ml of total gradient volume were collected. Proteins in each fraction were separated by SDS-PAGE and transferred to nitrocellulose membranes for immunoblotting with antibody specific for Sec8p and myc. In parallel, glycerol gradients were centrifuged containing globular protein standards with known sedimentation coefficients: bovine serum albumin (4.3S), β-amylase (11.2S), and thyroglobulin (19.2S).

Statistics

The sizes of cysts, the number of tubules per cyst, the synthesis of gp80, and the synthesis and surface delivery of E-Cadherin and gp135 were summarized by medians and the statistical significance assessed by the Mann-Whitney nonparametric test.

RESULTS

Exocyst Localizes to the Tight Junction and Relocalizes during Tubulogenesis

We have previously shown that during HGF-induced formation of tubules from MDCK cells grown as cysts, the cells go through a dramatic sequence of changes in polarity and shape (Pollack *et al.*, 1998). To investigate the possible role of the exocyst in these changes, we began by localizing the exocyst during this process. In MDCK cells grown as a monolayer on a filter support, the exocyst localized to the region of the tight junction (Grindstaff *et al.*, 1998). We first localized the exocyst in non-HGF–treated cysts, where the MDCK cells formed a polarized monolayer surrounding a lumen. Although the polarity of cells in a collagen gel cyst is generally thought to closely resemble that of filter-grown cells, proteins such as galectin-3 have been shown to be secreted apically in monolayers (Lindstedt *et al.*, 1993; Sato *et al.*, 1993) but basolaterally in cysts (Bao and Hughes, 1995, 1999). Compared with growth on a porous plastic filter, growth in an extracellular matrix gel is more likely to resemble the environment experienced by cells in vivo. Given the differences between filter-grown and cyst-grown cells, it was important to first examine the localization of the exocyst in cells grown as cysts.

We found that the exocyst localized to the tight junction in polarized MDCK cell cysts and colocalized with the tight junction marker ZO-1 (Figures 1 and 2, a–c). In addition to the tight junction staining, there was also diffuse cytoplasmic staining. This could represent intracellular exocyst, because even in fully polarized MDCK cells, previous investigators have shown that only ~70% of Sec6p and Sec8p migrated near the top of an Opti-Prep gradient with the plasma membrane protein E-cadherin, suggesting 30% remained cytosolic. This can be contrasted to nonpolarized MDCK cells in which >90% of Sec6p and Sec8p migrated to a position near the bottom of the gradient and was presumably cytosolic (Grindstaff *et al.*, 1998). We cannot, however, rule out the possibility that at least some of the cytoplasmic staining represented nonspecific background staining. It should be noted that diffuse background staining is often somewhat higher in a collagen gel system, due to the difficulties in thoroughly blocking and washing through the thick collagen gel, though this problem varies with the antibody used (e.g., the antibody to ZO-1 is clean even in cysts) (Pollack *et al.*, 1997, 1998).

During tubulogenesis cells undergo a series of steps of physiologic remodeling of cell polarity and shape. We investigated whether during tubulogenesis, changes in exocyst localization, corresponding to changes in cell polarity, would be seen. We have previously shown that in the first stage of HGF-induced tubule formation, the extension stage, basolateral extensions of individual cells protrude into the surrounding collagen matrix whereas the cells remain attached to the cyst. Cell polarity and cell junctions, however, are maintained (Pollack *et al.*, 1998). In this stage a substantial amount of the exocyst was found in the basolateral extension, and often seemed to be concentrated at the base of the extension. This may be analogous to cytoplasmic exocyst in contact-naive cells (Grindstaff *et al.*, 1998). However, some of the exocyst staining remained at the region of the tight junction (Figure 2, d–f).

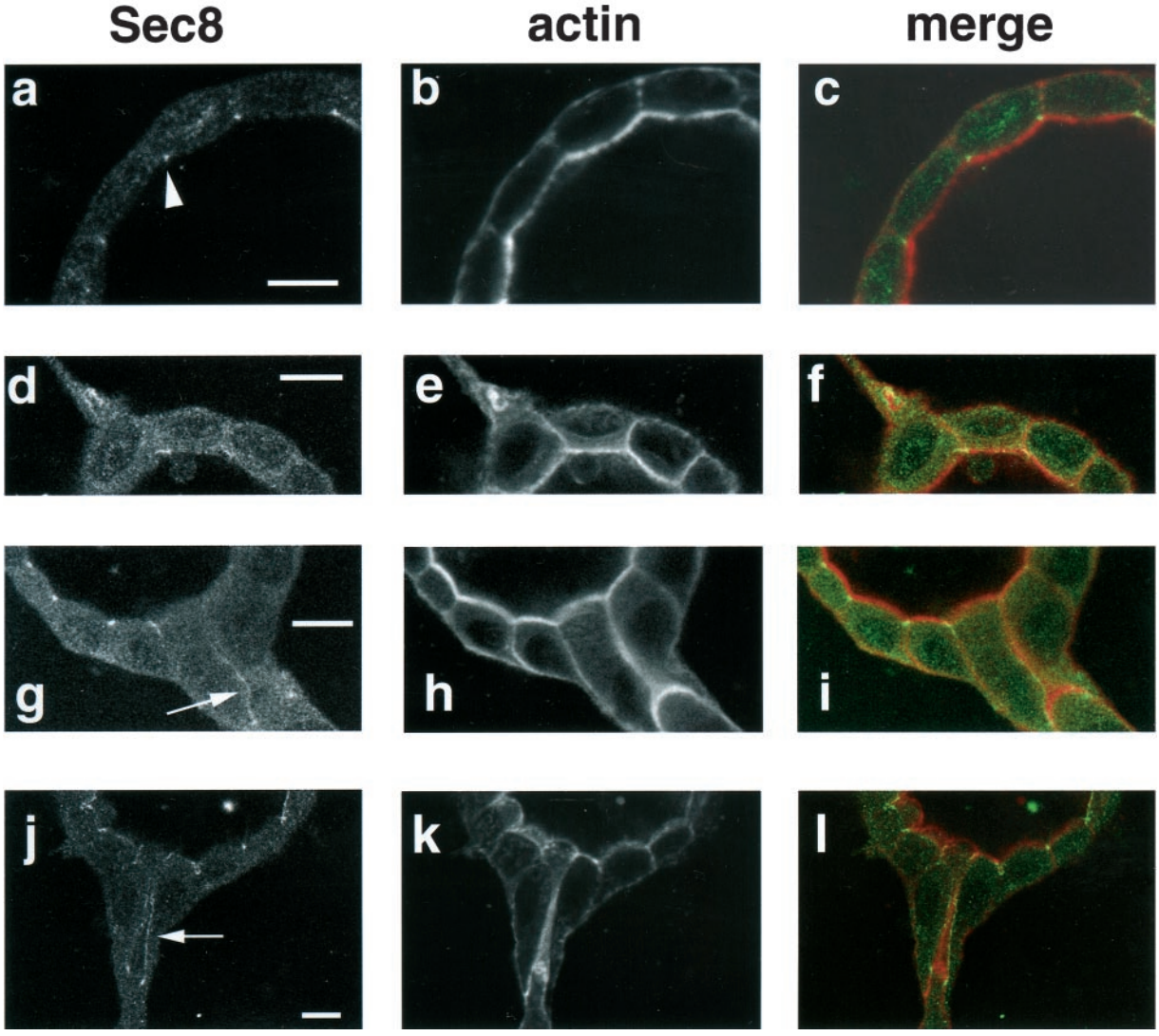

Figure 2. Sec8p relocalizes during tubulogenesis. (a and b) Fluid-filled cyst formed by MDCK cells grown for 10 d in a collagen gel. Staining is seen at the area of the tight junction (arrowhead) by using anti-Sec8 antibody (a). Sec8p colocalized with the tight junction protein ZO-1 (Figure 1). Concurrent staining of actin with phalloidin was performed (b). (c) Merge of a and b. (d–l) Fluid-filled cysts formed by MDCK cells grown for 10 d in collagen and stimulated for 24 h with conditioned medium containing HGF. The exocyst can be seen relocalizing along the growing tubules in a pattern consistent with the changes in polarity that occur as tubules form. (d–f) Extension stage of tubulogenesis. Sec8p is seen relocalizing into the extension (d), in association with actin staining (e). (g–i) Cord stage of tubulogenesis. Arrow in g indicates staining at the region of cell–cell contact in the cord. This region may become the boundary of a new lumen, as shown by the intense actin staining in this region (h). (j–l) Nascent tubule in the final stage of tubulogenesis. Arrow in j shows two vertical lines of Sec8p staining outlining the boundary of the lumen. Intense actin staining in a broad band in k underlies the apical surface surrounding this lumen. (f, i, and l) Merge of d and e, g and h, and j and k shows that the relocalizing exocyst closely surrounds, but does not precisely overlap the actin in the projections of the nascent tubules as indicated by lack of yellow in the merged panels. Sec 8, green; actin, red. Bar, 10 μm.

During a later stage, cells form cords that are groups of cells, two or three cells thick, that project away from, while retaining contact with, the cyst. These cords do not contain visible lumens, though nascent lumens may be forming at regions of cell–cell contact. We costained all of our samples for polymerized actin by using Alexa 594 phalloidin. Cortical actin underlies the entire plasma membrane; however, actin staining is particularly strong underneath apical surfaces and at regions of cell–cell contact that are likely to form future apical surfaces during the later stages of tubulogenesis. We have found the pattern of actin staining to be particularly helpful for visualizing the reformation of polarized cell structures during tubulogenesis (Pollack *et al.*, 1998). In the cord stage, the exocyst was expressed between areas of cell–cell contact, as shown by the arrow (Figure 2g) and the corresponding actin staining (Figure 2h). This seems analogous to a previous study showing that the exocyst went from a largely cytoplasmic state in contact-naive

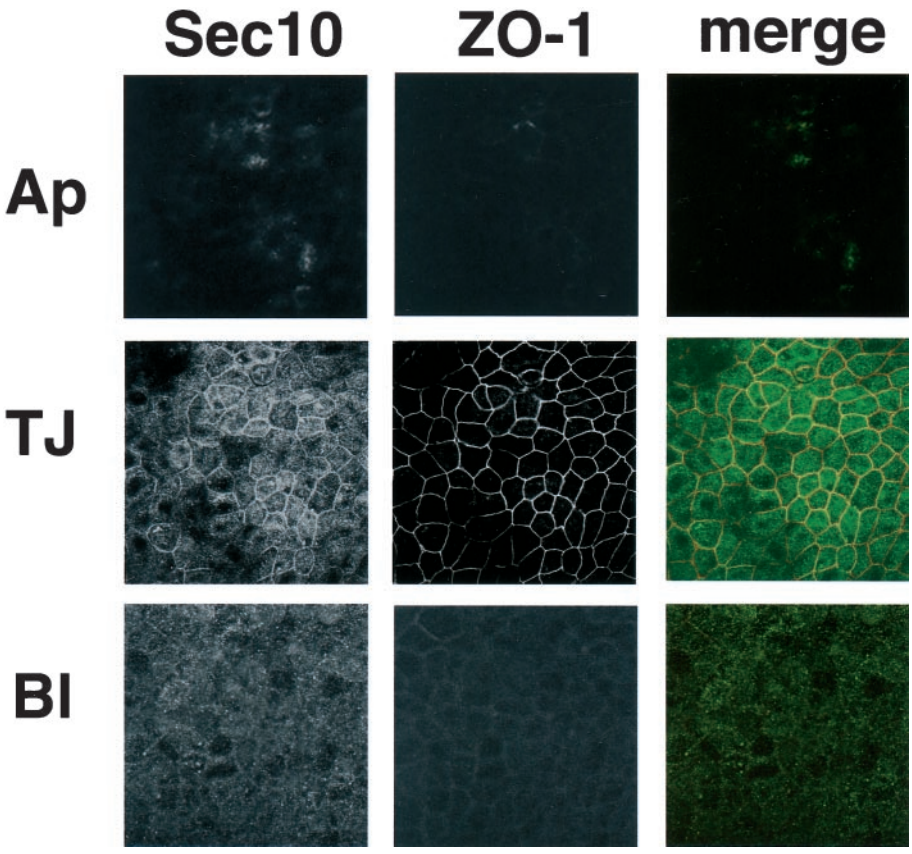

Figure 3. Sec10p partially localizes at the tight junction. Antibody against Sec10p and antibody against the tight junction marker ZO-1 demonstrated colocalization (yellow in merged panels) at the tight junction in MDCK cell monolayers grown for 7 d on filters. Ap, apical; TJ, tight junction; Bl, basolateral. Sec 10, green; ZO-1, red. Bar, 10 μm.

MDCK cells to localization at the area of cell–cell contact as polarity was initiated in early contact MDCK cells grown in two-dimensional cultures on filters (Grindstaff *et al.*, 1998).

During the final stage of tubulogenesis small lumens begin to appear along the length of the developing tubule. Tubule maturation then occurs with the individual lumens coalescing, enlarging, and becoming continuous with the lumen of the cyst. Apical and basolateral membranes of cells of the tubule become clearly polarized and the arrangement of cell junctions that normally is found in polarized epithelial cells is restored (Pollack *et al.*, 1998). The exocyst can be seen relocalizing during this final stage of tubulogenesis (Figure 2, j and k). A nascent lumen between cells, sectioned longitudinally, is indicated by the elongated band of strong actin staining, which is characteristically subjacent to the apical surface (Figure 2k). Two thin lines of Sec8 staining (arrow in Figure 2j) bracket this actin staining. The relocalization of the exocyst during tubulogenesis is highly suggestive of the redirection of delivery of new membrane and secretory products to the growing extensions and tubules during the physiologic remodeling of cell shape and polarity that occurs throughout the tubulogenic process. This relocalization is strikingly similar to the way in which the exocyst is involved in redirecting exocytic vesicles to different regions of the plasma membrane during the yeast cell cycle.

The exocyst surrounded, but did not overlap the actin extending into the tubular processes. Note the green lines of Sec8 staining (arrows in Figure 2, g and j) surrounding the thicker red actin staining (Figure 2, i and l). Studies from yeast demonstrate a strong connection between the exocyst and the actin cytoskeleton (Ayscough *et al.*, 1997; Finger and Novick, 1998). Although there are no reports to date that the exocyst and actin cytoskeleton interact in mammalian cells, there is increasing evidence that the actin and microtubule cytoskeletons cooperate in membrane traffic (Goode *et al.*, 2000). It is therefore plausible that the interactions of the exocyst with the actin cytoskeleton are important in directional vesicular traffic in MDCK cells.

A Portion of Overexpressed hSec10-myc Associates with the Rest of the Exocyst Complex

Only the localizations of Sec6p and Sec8p have previously been reported in MDCK cells (Grindstaff *et al.*, 1998). We examined the localization of endogenous canine Sec10p in MDCK cells. A significant portion of endogenous canine Sec10p (Figure 3) colocalized with ZO-1 at the tight junction. However, staining with the antibody to Sec10p had a broader distribution than staining for ZO-1, which was highly localized to the tight junction (Figure 3, TJ row). Some Sec10p staining was also intracellular, mainly in a diffuse cytosolic pattern (though there may be some unidentified puncta). We did not see any of this staining with nonimmune antibodies (Lipschutz and Mostov, unpublished observations). However, because we did not have control cells lacking Sec10p, we could not rule out the possibility that some of this staining was nonspecific background.

To better understand the role and localization of the exocyst in MDCK cells, we used the approach of overexpressing one subunit. We chose Sec10 because the Sec10 subunit has been shown to be part of a separate subcomplex consisting of Sec10p and Sec15p, and perturbation of Sec10 function in yeast has specific effects on polarized vesicular delivery (Roth *et al.*, 1998; Guo *et al.*, 1999b). We recently cloned hSec10 (Guo *et al.*, 1997). Full-length hSec10 was transfected into MDCK cells and clones expressing hSec10 were selected. Three clones, expressing differing levels of hSec10, were chosen for further study (Figure 4a). In the following experiments all three clones showed similar phenotypes, and, in all the cases where quantitative data are presented, the differences from control cells transfected with vector alone were statistically significant. There seemed to be a rough, though not absolute, correlation between the level of hSec10 overexpression and the magnitude of the effects seen; however, given the small number of hSec10 overexpressing clones examined thoroughly, we cannot make any definitive statements. We estimate the degree of expression of transfected hSec10p over endogenous canine Sec10p to be approximately three- to fivefold in the clone expressing the highest amount of hSec10 (Lipschutz and Mostov, unpublished observations).

To circumvent the possible background staining problem and to investigate the distribution of the transfected hSec10p without the fluorescence signal from endogenous canine Sec10p, we stained cells for the myc epitope present on the transfected hSec10p (Figure 4b). Immunofluoresence staining with antibody against the myc epitope tag showed transfected hSec10p mainly at the tight junction region, which was identified by costaining for ZO-1 (Lipschutz and Mostov, unpublished observations). Some hSec10p was again present intracellularly, mostly diffusely in the cytosol (Figure 4b). The level of background staining with control cells was very low, so we are confident that this signal was due to the transfected hSec10p. Therefore, Figures 3 and 4 taken together suggest that both endogenous Sec10p and the transfected hSec10p have significant localization to the tight junction region, as well as some intracellular localization.

At steady state, in polarized cells grown on filters there was no difference in the levels of Sec6p and Sec8p, per microgram of total protein, in hSec10 transfected cells compared with control cells (Figure 4c) and Sec6p and Sec8p continued to localize at the tight junction in hSec10 overexpressing cells (Lipschutz and Mostov, unpublished observations).

Previous investigators have shown that the eight-member exocyst complex sedimented at ~17S. Although Sec6p sedimented as a reasonably symmetric peak centered around 17S, Sec8p was shown to have a much broader distribution, including a wide shoulder sedimenting around ~11S, which may represent a subset of proteins in a partially assembled or disassembled complex (Grindstaff *et al.*, 1998). We found that the sedimentation of hSec10p largely paralleled that of endogenous Sec8p. Specifically, 72% of the overexpressed hSec10p sedimented with the same velocity as 90% of the endogenous Sec8p (Figure 5a). Of course, this result does not establish that any or all of the hSec10p that sediments at the same rate is truly physically associated with the Sec8p. Moreover, hSec10p had an overall distribution that was slightly shifted to a slower sedimentation, suggesting that some of the hSec10p may be in a smaller complex(es) or form(s) than Sec8p.

To determine how much of the hSec10p was associated with the endogenous Sec8p, we used a coimmunoprecipitation protocol, which is explained in detail in MATERIALS AND METHODS. We immunoprecipitated Sec8p by using anti-Sec8 antibody. We found that four consecutive rounds of immunoprecipitation were sufficient to immunoprecipitate 81% of the Sec8p. A fifth and final round of immunoprecipitation was performed with antibody against the myc epitope tag. All of the immunoprecipitates were analyzed by SDS-PAGE and Western blot by using antibodies against Sec8p and the myc epitope tag of hSec10p. This procedure allowed us to accurately quantitate the amount of hSec10p that coimmunoprecipitated with Sec8p. Of the total hSec10p precipitated, 65% remained after Sec8p depletion (Figure 5b, □), suggesting the majority of transfected hSec10p was not complexed with the rest of the exocyst (Figure 5b). This is as expected, since the transfected hSec10p is predicted to be in excess over the endogenous Sec8p.

In the reciprocal experiment, we immunoprecipitated hSec10p via its myc tag. Four rounds of immunoprecipitation with antibody to the myc tag on hSec10p were sufficient to immunoprecipitate 86% of the hSec10p. A fifth and final round of immunoprecipitation was performed with antibody to Sec8p. Of the total Sec8p precipitated, only 35% remained after hSec10p depletion (Figure 5c, ■), indicating that the majority of endogenous canine Sec8p was complexed with the overexpressed hSec10p.

Taken together, these data show that ~35% of the overexpressed hSec10p associates with the Sec8p complex. It should be kept in mind that dissociation may occur during the lengthy sequential immunoprecipitations, which may result in an underestimation of the true degree of association. This association could be the mechanism by which the effects of overexpressed hSec10, described below, are mediated; however, it is certainly possible that free hSec10p is acting independently of the complex containing Sec8p. We were unable to express the carboxy- or amino-terminal domains of hSec10 in either a stable or an inducible system in MDCK cells, most likely due to their extreme toxicity.

Transfection with hSec10 Leads to Changes in Cell Morphology

When grown as a monolayer on filters, the cells overexpressing hSec10 were noted to be significantly taller in comparison with control cells both by confocal (13.9 ± 1.0 versus 10.1 ± 0.7 μm, as measured from the tight junction to the basal surface) and EM (Figure 6a, hSec10 overexpressing cells, and b, control cells). The number of cells growing per surface area of Transwell filter substrate, however, was unchanged (Lipschutz and Mostov, unpublished observations). Consistent with this, the mean diameter of hSec10 overexpressing and control cells appeared similar on EM (43.9 ± 9.4 μm/section versus 40.6 ± 10.5 μm/section), suggesting that cells are taller but not wider.

By EM the number of 50–100-nm vesicles seen within 500 nm of the plasma membranes was increased in the hSec10 transfected versus control cells both apically (0.305 ± 0.143 versus 0.050 ± 0.055 vesicles/μm of plasma membrane) and basolaterally (0.164 ± 0.067 versus 0.038 ± 0.033 vesicles/μm of plasma membrane) (Figure 6c, hSec10 overex-

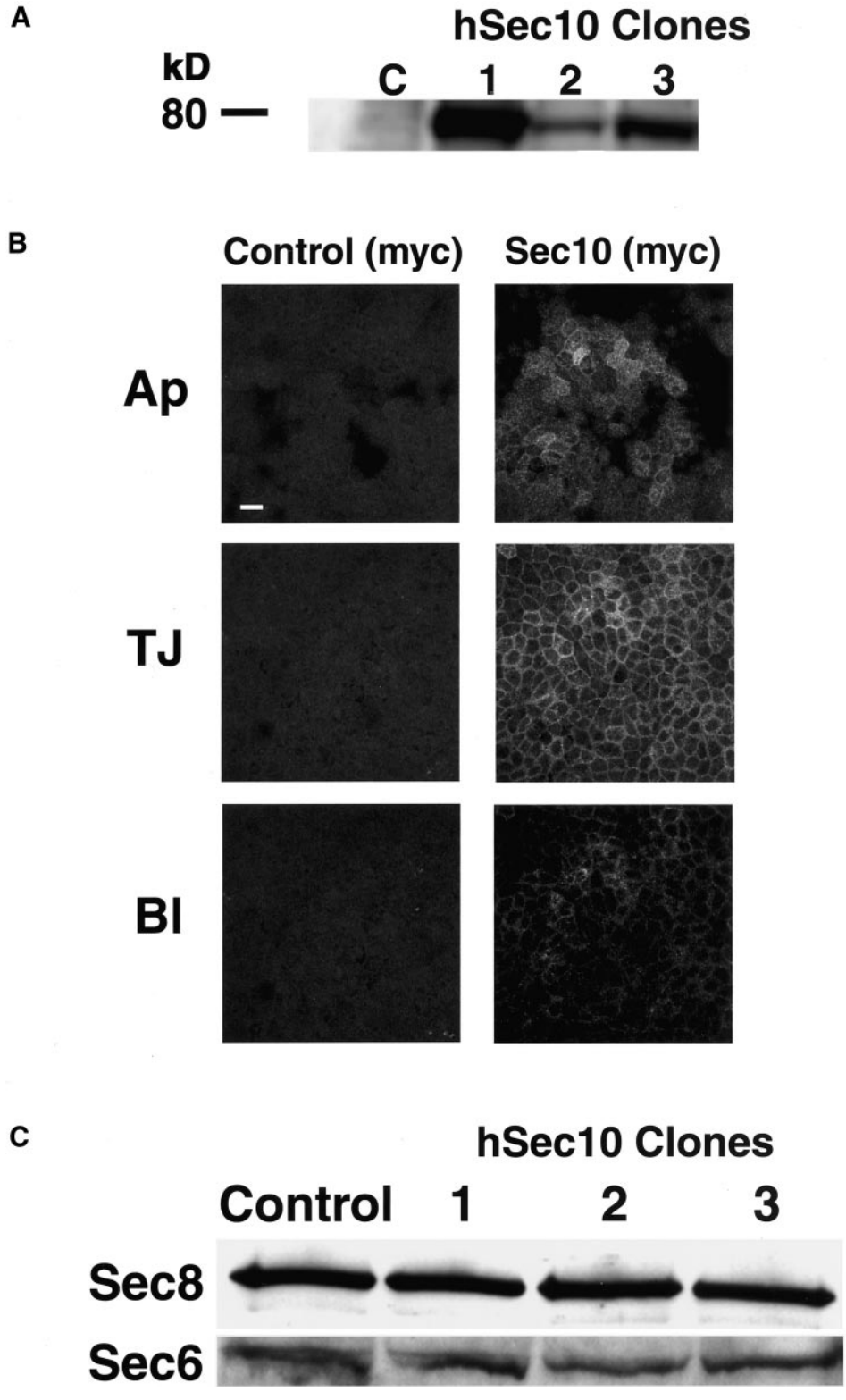

Figure 4. hSec10-myc partially localizes at the tight junction and the levels of Sec6p and Sec8p are unchanged in hSec10 overexpressing cells. (a) Western blot by using antibody against the myc epitope tag demonstrated three hSec10 expressing clones. C, control. (b) Immunofluorescent staining by using antibody against the myc epitope tag in hSec10 overexpressing cells shows transfected hSec10p localized to the plasma membrane at the level of the tight junction (the level of the tight junction was determined by costaining with ZO-1; Lipschutz and Mostov, unpublished observations). No myc staining is evident in the control cells. (c) Western blot demonstrates equal amounts of Sec6p and Sec8p protein per microgram of total protein in Sec10 overexpressing and control cells. Ap, apical; TJ, tight junction; Bl, basolateral. Bar, 10 μm.

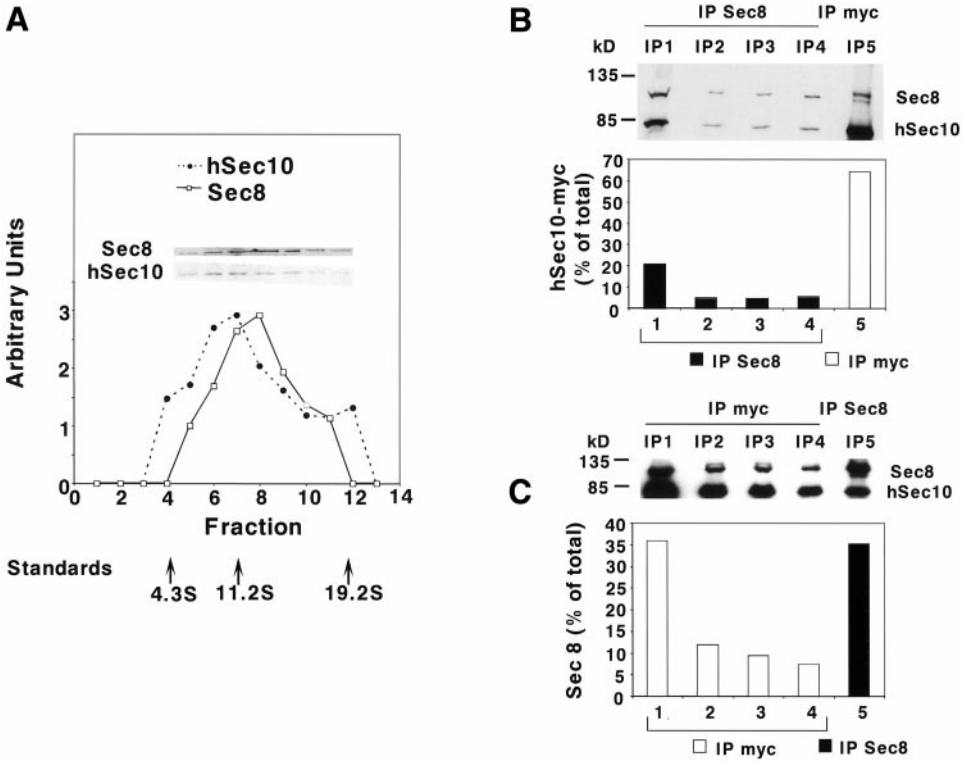

Figure 5. Partial association of Sec8p and hSec10p. (a) Glycerol gradient from homogenized cells overexpressing hSec10, with Western blot performed on each fraction by using antibody against Sec8p and the myc epitope tag of hSec10p. Size markers (arrows) are bovine serum albumin (4.3S), β-amylase (11.2S), and thyroglobulin (19.2S). (b) Four sequential immunoprecipitations by using antibody against Sec8p followed by an immunoprecipitation with antibody against the myc epitope tag on the transfected hSec10p demonstrated that 65% of the transfected hSec10p is not in a complex with endogenous Sec8p. Blotting was performed by using antibody against the myc epitope tag (blotting was also done with antibody against Sec8p to confirm depletion). Note that there is a doublet of ~116 and 120 kDa in the fifth immunoprecipitation. The upper band (120 kDa) of the doublet is a nonspecific contaminant seen in immunoprecipitations with antibody to myc (Lipschutz and Mostov, unpublished observations). The lower band (116 kDa) is a small amount of Sec8p that has escaped the first four rounds of immunoprecipitation, but is assumed to be associated with hSec10p as it was coimmunoprecipitated with hSec10p in the fifth round. (c) Four sequential immunoprecipitations by using antibody against the myc epitope tag followed by an immunoprecipitation with anti-Sec8 antibody demonstrated that 35% of the endogenous Sec8p was not complexed with the transfected hSec10p. Blotting was performed by using antibody against Sec8p (blotting was also done with antibody against myc to confirm depletion).

pressing cells, and d, control cells). The number of vesicles labeled during a 10-min exposure to extracellular apical and basolateral media containing HRP was the same in hSec10 transfected and control cells (Lipschutz and Mostov, unpublished observations), indicating that the increased number of vesicles was not a result of enhanced endocytosis. This suggested that the increased number of vesicles seen within 500 nm of the plasma membranes might represent increased numbers of vesicles involved in exocytosis at the surfaces. This prompted us, in the next set of experiments, to examine the effects of hSec10 overexpression on secretion.

Transfection with hSec10 Leads to Increased Synthesis and Delivery of Secretory and Basolateral, but not Apical, Plasma Membrane Proteins

Because the exocyst is involved in secretion in yeast, we decided to directly examine the effects of hSec10 transfection on protein delivery to the plasma membrane by performing pulse-chase experiments. gp80 is secreted apically and basolaterally and is the most abundant endogenous secretory protein in MDCK cells (Urban *et al.*, 1987). We first examined the steady-state level of gp80 associated with the cells by solubilizing the entire cell monolayer and analyzing by SDS-PAGE and Western blot with antibody to gp80. We found that the steady-state level of gp80, per microgram of total protein, was increased two- to threefold over control in all of the hSec10 overexpressing clones (Figure 7a).

For the experiments described next, all three hSec10 transfected clones showed similar results though due to space considerations we present the data for clone 1 only. We examined the rate of synthesis of gp80 by metabolically pulse labeling with [^{35}S]methionine for 20 min and then immunoprecipitating gp80 and analyzing by SDS-PAGE. The amount of gp80 synthesized was quantitated by using a phosphorimager. We found that the amount of gp80 synthesized was significantly increased (Figure 7b). We then examined apical and basolateral secretion of gp80 by metabolically pulse labeling with [^{35}S]methionine for 20 min and then chasing for 120 min, to allow the gp80 to be secreted into the apical and basolateral media. The media were analyzed by SDS-PAGE and the amount of secreted radioactive gp80 quantitated by phosphorimaging. We found that the secretion of gp80 into both the apical and basolateral media was increased two- to threefold in hSec10 overexpressing versus control cells (Figure 7, d and f).

To determine whether other secretory proteins also exhibited a similar increase in secretion in hSec10 transfected cells, we performed a similar metabolic label pulse-chase experiment and analyzed the apical and basolateral media by SDS-PAGE and phosphorimaging (Figure 7c). This enabled us to examine the entire profile of all major endogenous

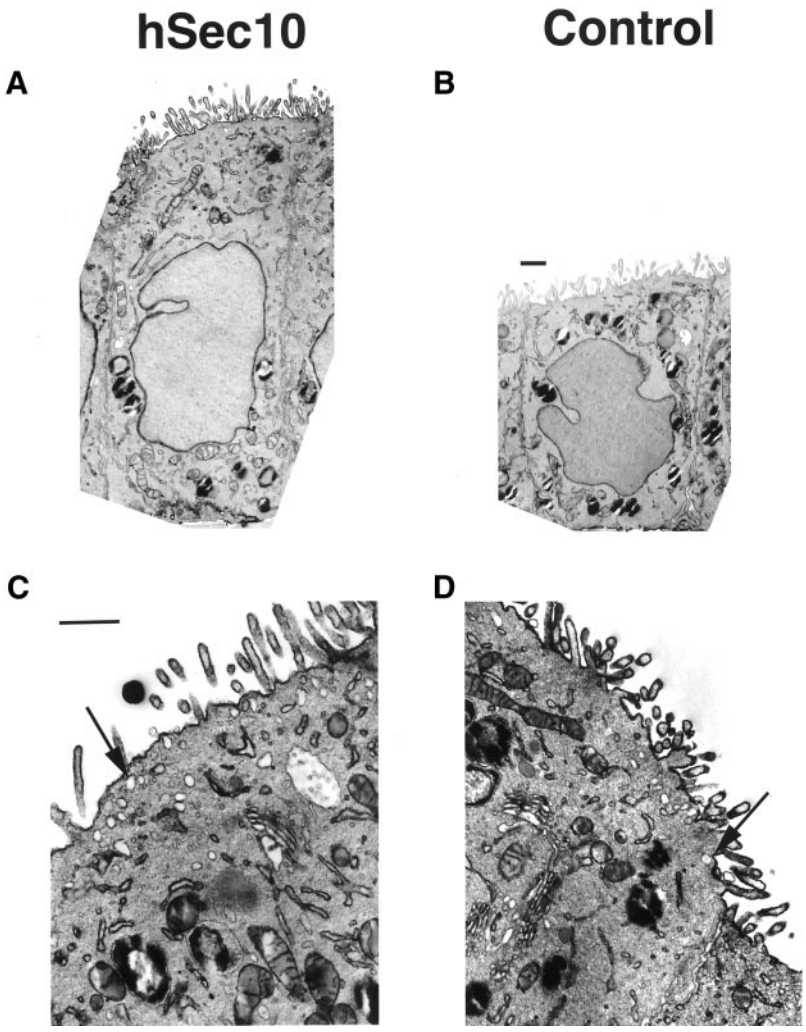

Figure 6. Morphological changes in hSec10 overexpressing cells, as shown by EM. (a and b) hSec10 overexpressing cells were vertically elongated (a) compared with control cells (b). (c and d) Increased numbers of vesicles were seen at the apical plasma membrane in hSec10 overexpressing cells (c) compared with controls (d). Increased numbers of vesicles were also seen basolaterally (Lipschutz and Mostov, unpublished observations). Arrows point to examples of 50–100-nm vesicles found within 500 nm of the plasma membrane. a and b and c and d were taken at equal magnifications. Bar, 1 μm.

secretory proteins. We determined the total amount of metabolically labeled proteins that were secreted apically and basolaterally by summing the amount of radioactivity in the appropriate lanes and found that the total amount of proteins secreted both apically and basolaterally was increased in hSec10 transfected cells (apical, 2167 $\pm$ 507 versus control, 761 $\pm$ 30; basolateral, 415 $\pm$ 66 versus 295 $\pm$ 41 arbitrary units) (Figure 7c). We did not detect a significant selective increase in any particular secretory protein, but rather a consistent pattern of increase for all secreted proteins.

Finally, we examined the effects of hSec10 expression on the kinetics of secretion. For this we focused again on gp80 because we could measure the total amount of gp80 synthesized. We found that the kinetics of secretion, i.e. the percentage of total gp80 secreted per unit time, were unchanged (Figure 7, e and g). Very little g80 was detected inside the cells after a 60-min chase, consistent with a previous report showing no intracellular storage of gp80 in MDCK cells (Appel *et al.*, 1996).

In addition to soluble secretory proteins, we examined representative integral membrane proteins of the basolateral and apical surface. E-Cadherin is a basolateral plasma membrane protein, whereas gp135 is an apical plasma membrane protein (Yeaman *et al.*, 1999). Pulse-chase in combination with surface biotinylation demonstrated that cells overexpressing hSec10 synthesized more E-Cadherin and delivered more to the basolateral plasma membrane, but neither synthesized more gp135 nor delivered more to the apical surface (Figure 8).

These results show that overexpression of hSec10 affects not only membrane traffic but also, surprisingly, synthesis of certain proteins, including at least one endogenous basolateral membrane protein and a whole spectrum of apical and basolateral secretory proteins. Transcytosis of IgA by transfected polymeric immunoglobulin receptor was unchanged in hSec10 overexpressing versus control cells (Lipschutz and Mostov, unpublished observations), suggesting that transcytosis is not a pathway influenced by the exocyst.

Transfection with hSec10 Leads to Increased Cystogenesis and Tubulogenesis

When MDCK cells are seeded as sparse single cells in a three-dimensional collagen gel, the cells multiply and over a period of ~10 d form hollow spherical cysts. These

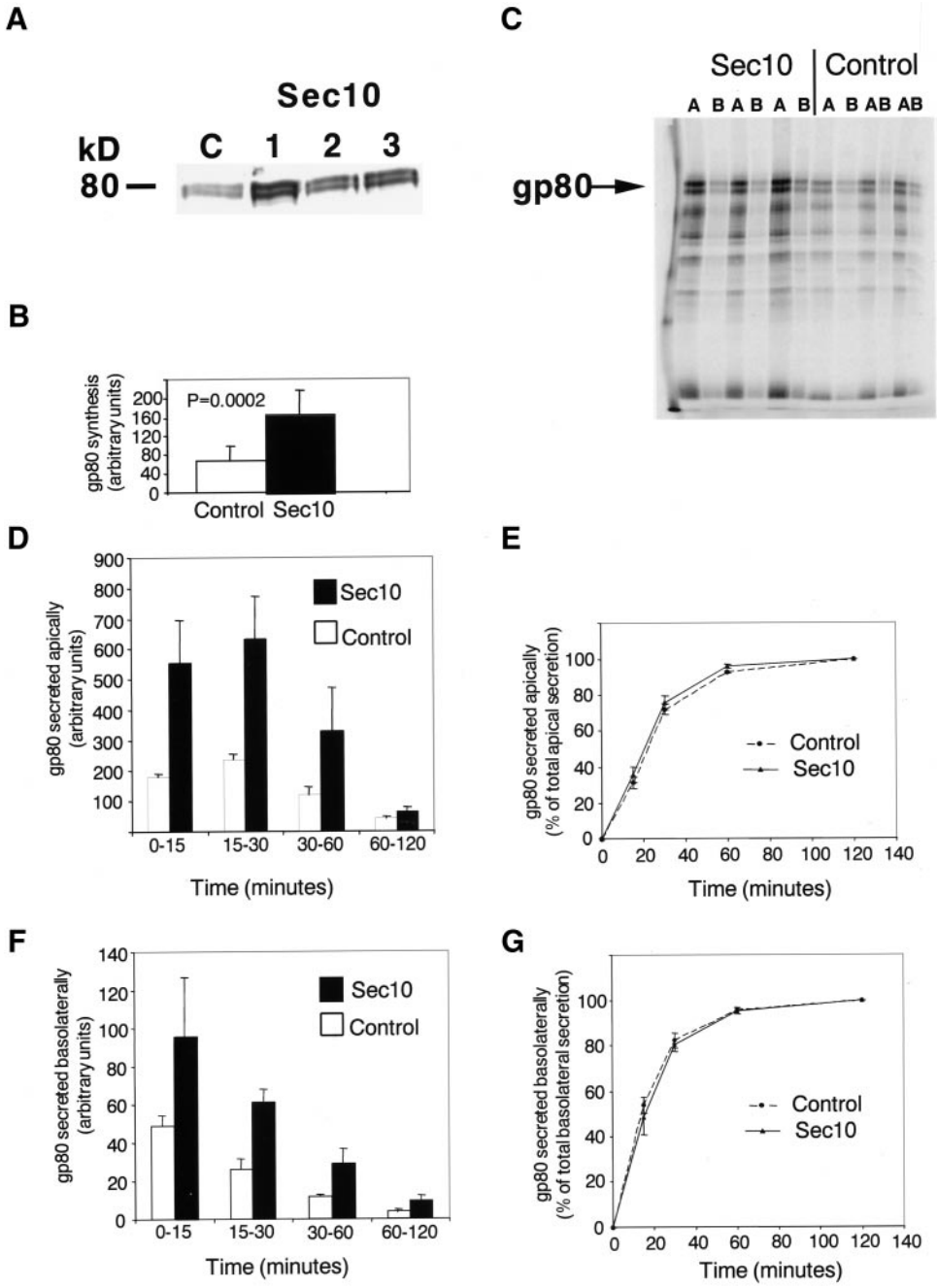

Figure 7. Synthesis and delivery of secretory proteins in hSec10 overexpressing cells. (a) Western blot by using antibody against gp80 demonstrates increased steady-state levels of gp80 in three hSec10 transfected clones (1, 2, 3) compared with control cells (C). (b–g) Synthesis and secretion assays were performed by pulse and pulse-chase with [^{35}S]methionine. (b) hSec10 overexpressing and control cells were metabolically pulse labeled for 20 min with [^{35}S]methionine and the amount of newly synthesized gp80 was measured. (c) Other secretory proteins were also increased in hSec10 overexpressing versus control cells. Cells were pulse labeled for 20 min with [^{35}S]methionine, and chased for 1 h. Then the apical (A) and basolateral (B) media were collected and aliquots run on SDS-PAGE and analyzed by phosphorimaging. The entire gel is shown and the position of gp80 indicated by the arrow. We show this experiment in triplicate to demonstrate that even though there is some variability, there is a general consistency with respect to the increase in apical and basolateral protein secretion across a broad spectrum of secretory proteins. (d and f) hSec10 overexpressing and control cells were metabolically pulse labeled for 20 min. The apical and basolateral media were collected for the indicated time intervals during the subsequent chase. Aliquots were analyzed by SDS-10% PAGE and radioactivity associated with gp80 was determined by using a phosphorimager. Total secretion of gp80 was increased both apically (d) and basolaterally (f). (e and g) Data in d and f were replotted in e and g, respectively, to emphasize the kinetics of secretion, i.e., the fraction of the total gp80 secreted as a function of time. Data for each condition were normalized, so that the total gp80 secreted into the apical (e) or basolateral (g) media by the end of the 120-min time course was taken as 100%. The cumulative secretion at each time point was then plotted. These results indicate that although the amounts of gp80 secreted apically and basolaterally were increased by hSec10 transfection, the kinetics of secretion, measured as cumulative percent of total over time, was unchanged.

cysts are polarized with the apical surface facing the fluid-filled interior. This is a model for the formation of cysts, which are one of the basic building blocks of higher order organizations of epithelial cells used in organogenesis. We wished to investigate the role of the exocyst in this process. When hSec10 overexpressing cells were plated at very low density in collagen gels (Montesano *et al.*, 1991a,b) they formed cysts more efficiently and at a significantly greater rate than did control cells (Figure 9, a–c). All three clones of hSec10 overexpressing cell cysts were larger and had a greater diameter than control cell cysts (i.e., clone 1, median diameter 90 versus 70 μm, $p < 0.0001$), though the cell number was unchanged (Lipschutz and Mostov, unpublished observations). The larger

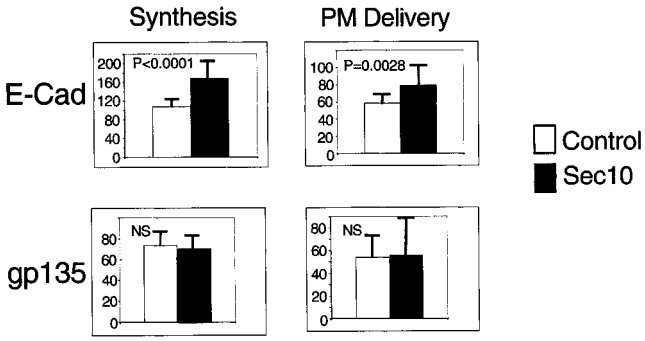

Figure 8. Synthesis and delivery of plasma membrane proteins in hSec10 overexpressing cells. In contrast to gp135, E-Cadherin synthesis and delivery were increased in hSec10 overexpressing versus control cells. The p values were the result of at least three experiments and were determined by the Mann-Whitney nonparametric test. Units are arbitrary phosphorimager units. NS, nonsignificant. Sec10 (■), control (□).

cyst size is consistent with the taller cell size measured previously (Figure 6, a and b).

When MDCK cell cysts grown in collagen as described above are then exposed to HGF, the cysts form branching tubules that extend out from the cyst. This is a model for the formation of tubules, another of the basic types of higher order organization of epithelial cells used in organogenesis. To investigate the possible role of the exocyst in tubulogenesis, we studied this process. After 48 h of HGF stimulation, we quantitated the extent of tubulogenesis by counting the number of visible tubules at the area of greatest cyst diameter. Cysts were grouped into bins containing 0–4, 5–9, 10–19, and 20+ tubules per cyst. Most remarkably, when induced by HGF, all three clones of the cysts composed of hSec10 overexpressing cells formed significantly more tubules per individual cyst compared with controls (Figure 10, a–c).

DISCUSSION

We report two principal findings, both of which are surprising. First, we show that the exocyst is centrally involved in cystogenesis and tubulogenesis. We found that the exocyst relocalized during tubulogenesis coincident with changes in polarity. Transfection of the hSec10 component of the exocyst led to a gain of function phenotype that included more efficient and rapid cyst formation and increased tubulogenesis upon stimulation with HGF. Second, this gain of function also included the unexpected increase in synthesis of at least one basolateral plasma membrane protein, as well as a whole array of both apical and basolateral secretory proteins.

In mice, a mutation in an exocyst subunit (Sec8) resulted in early embryonic lethality, which is understandable given the importance of the exocyst to the exocytic machinery (Friedrich *et al.*, 1997; Hsu *et al.*, 1998). Unlike the Sec8 gene disruption, the relocalization of the exocyst during tubulogenesis, the accelerated formation and increased diameter of cysts overexpressing hSec10, and the increased number of tubules with hSec10 overexpression indicate a more specific and unexpected involvement of the exocyst in cystogenesis and tubulogenesis. Cysts and tubules represent two of the basic building blocks of higher order organizations of epithelial cells used in organogenesis and the specific role of the exocyst offers an important new insight into these vital, yet poorly understood, processes.

Basolateral extensions represent the first stage of tubulogenesis (Pollack *et al.*, 1998). It seems probable that these extensions are dependent on the synthesis and delivery of secretory and plasma membrane proteins to the basolateral surface in a manner analogous to cell locomotion likely depending on exocytosis and recycling at the leading edge of a crawling fibroblast (Bretscher and Aguado-Velasco, 1998). This could be the mechanism for increased tubulogenesis seen with hSec10 transfection. The relocalization of the exocyst during tubulogenesis is reminiscent of the developmentally programmed delivery of new membrane proteins to very specific locations during epithelial formation in the *Drosophila* embryo (Lecuit and Wieschaus, 2000). The enhanced cystogenesis in the hSec10 overexpressing cell cysts could be a direct result of increased apical secretion into the cyst lumen, and/or increased synthesis of basolateral plasma membrane proteins. It is interesting to note that the yeast exocyst is involved in transport of vesicles to the bud and in MDCK cells the exocyst is involved in transport of vesicles to the basolateral surface. The analogy of the relationship of the bud to the basolateral surface is further

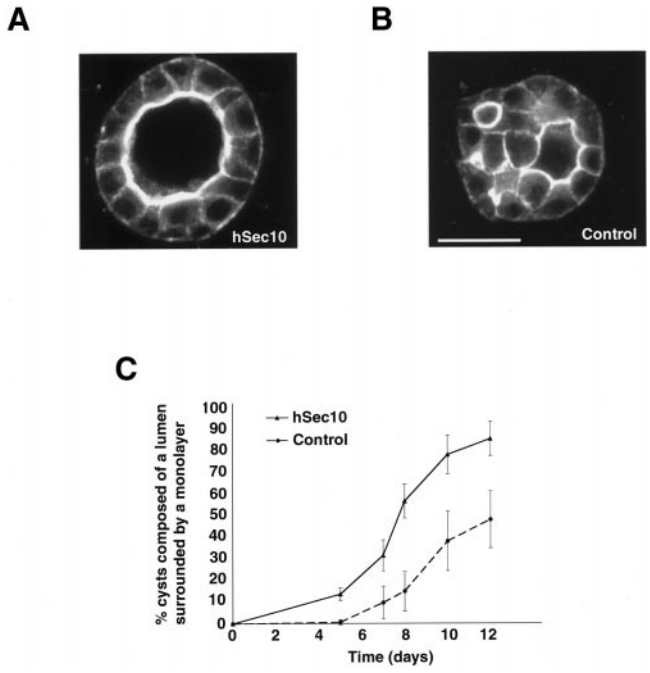

Figure 9. Effect of hSec10 overexpression on cystogenesis. (a and b) After 7 d of growth in a collagen matrix, cysts composed of hSec10 transfected cells (a) were mature, while cysts composed of control cells (b) were incompletely formed (confocal microscopy, cysts were stained for actin with phalloidin). (c) Quantitation demonstrated the increased rate and efficiency of mature cyst formation, as noted in a and b, in hSec10 overexpressing compared with control cell cysts. a and b were taken at equal magnification. Bar, 30 μm.

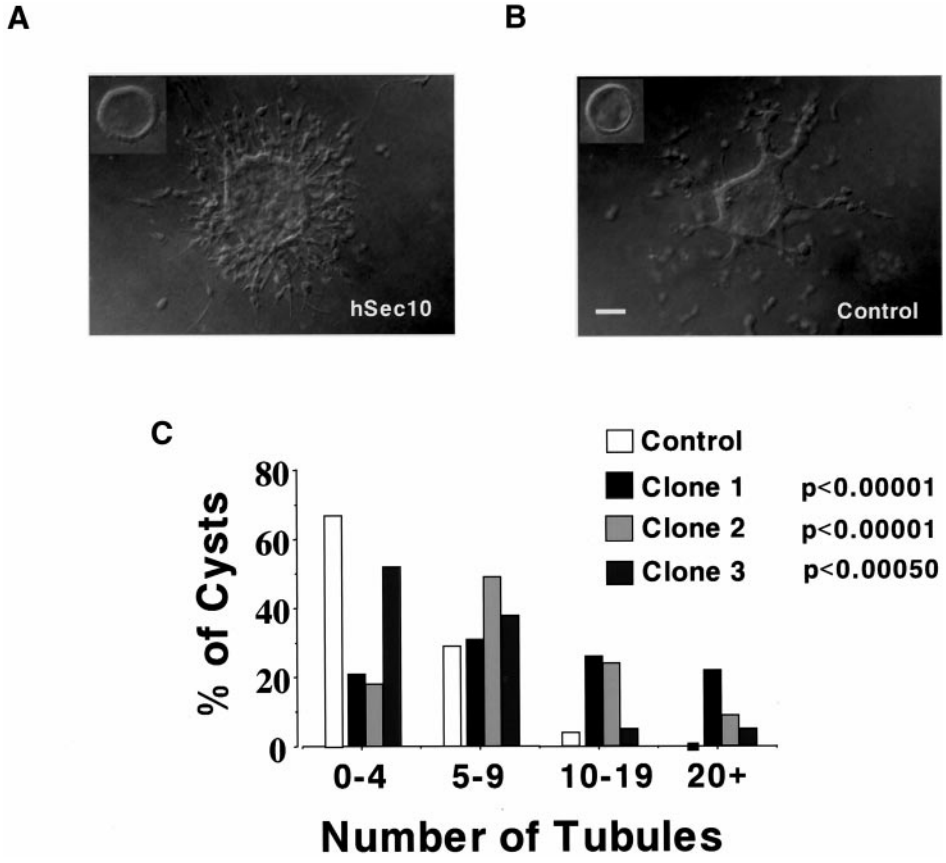

Figure 10. Effect of hSec10 overexpression on tubulogenesis. (a and b, insets) Nomarski imaging of mature hSec10 overexpressing (a, inset) and control (b, inset) cell cysts grown for 10 d in collagen again showed that the cysts composed of hSec10 overexpressing cells were larger than cysts composed of control cells. (a and b) HGF-induced stimulation, for 48 h, of mature cysts revealed greater numbers of tubules per cyst in the cysts composed of hSec10 overexpressing (a) versus control cells (b). (c) Quantitation of the number of tubules formed per cyst, as measured at the level of greatest cyst diameter, revealed increased tubulogenesis in all the clones of hSec10 overexpressing versus control cell cysts. Similar effects were seen as early as 6 and 12 h after addition of HGF (Lipschutz and Mostov, unpublished observations), indicating that the increase in tubule number was not simply a result of enhanced tubular lumen formation, which is a later event (Pollack *et al.*, 1998). a and b were taken at equal magnification. Bar, 30 μm.

supported by the role of Cdc42. Yeast cells expressing defective *CDC42* alleles do not form buds but, instead, appear to grow in a nonpolarized manner (Adams *et al.*, 1990), and inhibition of Cdc42 function in MDCK cells prevents delivery to the basolateral surface (Kroschewski *et al.*, 1999).

We suggest that the increase in secretory and basolateral plasma membrane protein synthesis resulting from hSec10 overexpression involves a signaling pathway whereby events involving exocytosis somehow influence protein synthesis, essentially a feedback loop connecting exocytosis and synthesis. An analogous system may be the increased synthesis of dense core granule components after degranulation in *Tetrahymena* (Haddad and Turkewitz, 1997). The effects of hSec10p transfection might be direct or indirect at any step that regulates gene expression, such as transcription, movement into or out of the nucleus, mRNA stability, or translation. Sec10p and the rest of the exocyst are concentrated at the tight junction in polarized MDCK cells. Although it is not yet known what proteins the exocyst interacts with, several tight junction proteins such as ZO-1, ZO-2, and ZO-3, contain the membrane-associated guanylate kinase domain, which is potentially involved in signaling (Butz *et al.*, 1998; Haskins *et al.*, 1998). Indeed it has been suggested that the tight junction is a signaling center (Li and Mrsny, 2000). It is tempting to speculate that either part of the exocyst (perhaps Sec10p or another subunit) or a protein that interacts directly or indirectly with the exocyst can translocate to the nucleus and act on transcription. Although ZO-1 is not known to interact directly with the exocyst, the presence of both in the tight junction region raises the possibility of an interaction, albeit perhaps an indirect interaction. Moreover, ZO-1 has been shown to localize to the nucleus in subconfluent but not confluent epithelial cells (Gottardi *et al.*, 1996). Additionally, ZO-1 has been shown to interact with the Y-box transcription factor ZONAB, in the regulation of the ErbB-2 promoter in a cell-density–dependent manner (Balda and Matter, 2000). There are now several examples of proteins at the cell surface that also influence nuclear events. For instance, β-catenin moves from the lateral surface of the cell to the nucleus and influences transcription (Korinek *et al.*, 1997; Morin *et al.*, 1997; Peifer, 1997; Rubinfeld *et al.*, 1997). Other examples include STAT (Leonard and O'Shea, 1998), SMAD transcription factors (Kretzschmar and Massague, 1998), and c-Abl (Lewis *et al.*, 1996). In another variation, EPS15, a component of clathrin-coated pits affects nucleocytoplasmic transport (Doria *et al.*, 1999). Recently, CASK, a membrane-associated guanylate kinase protein enriched at neuronal cell junctions, was shown to translocate to the nucleus and interact with T-brain-1, a T-box transcription factor, to regulate transcription (Bredt, 2000; Hsueh *et al.*, 2000). Finally, the junctional protein p120 catenin interacts with the transcription factor Kaiso (Daniel and Reynolds, 1999) and also acts more directly on the cytoskeleton through the Rho family exchange factor Vav2 (Noren *et al.*, 2000). This last example illustrates how a junction-associated protein can influence diverse sig-

naling pathways in the cell, which may also be the case for Sec10p.

Our data, as well as that of Grindstaff *et al.* (1998) suggest that there may be at least two pathways to the apical surface. One pathway carries at least certain apical membrane proteins such as gp135 and exogenously expressed $p75^{NTR}$ and the exocyst does not seem to play a role in this pathway. Another pathway involves a broad array of secretory proteins and this pathway does involve the exocyst, at least in that overexpression of hSec10 increases their synthesis. This is consistent with other recent evidence showing multiple pathways from the trans-Golgi network to the apical surface of MDCK cells (Mostov *et al.*, 2000; Orzech *et al.*, 2000).

The effects of hSec10 overexpression on cyst and tubule formation are reminiscent of ADPKD. ADPKD is one of the most common potentially lethal genetic disorders in humans, inherited as a dominant trait, and results in cystic and tubular overgrowth, which leads to destruction of the normal kidney architecture and renal failure (Grantham, 1997). In ADPKD there are gross abnormalities in cell polarity in the cells lining the gigantic cystic expansions of the tubules (Wilson *et al.*, 1991; Avner *et al.*, 1992; Gabow, 1993). For example, there is reversed polarity of Na^+-K^+-ATPase, with mislocalization to the apical plasma membrane in ADPKD epithelia (Wilson *et al.*, 1991). Although the *PKD1* and *PKD2* genes (Consortium, 1995; Mochizuki *et al.*, 1996), which when mutated are responsible for the vast majority of cases of ADPKD, have been identified, their function, role in cystogenesis and tubulogenesis, and downstream effectors remain largely unknown (Arnould *et al.*, 1999). In ADPKD, cysts develop from renal tubular epithelial cells (Grantham, 1997). MDCK cells are also derived from renal tubular epithelium (Simons and Fuller, 1985). Recent work demonstrates exocyst abnormalities in ADPKD cells. In normal kidney cells both Sec6p and Sec8p were localized in close apposition to the tight junction protein occludin. In contrast, both proteins were depleted from the ADPKD cell lateral membranes and appeared diffusely dispersed throughout the cytoplasm (Charron *et al.*, 2000). This is analogous to the cytoplasmic localization of Sec6p and Sec8p in contact-naive MDCK cells (Grindstaff *et al.*, 1998), suggesting that the defect in ADPKD cells lies in their response to cell–cell contact.

It is worthwhile to compare our results to recent progress in analysis of tubulogenesis in genetically tractable organisms. The trachea of *Drosophila* has been well studied and a number of genes and proteins have been identified that control morphogenesis of this structure (Metzger and Krasnow, 1999). In both *Drosophila* trachea and the renal system of *Caenorhabditis elegans*, a number of mutants have been isolated that affect the diameter of tubules, though most of these genes have yet to be cloned (Buechner *et al.*, 1999; Beitel and Krasnow, 2000). The phenotype of some of these mutants is similar to the increase in cyst diameter that we observe upon overexpression of hSec10.

Our results provide an entirely new perspective with respect to the exocyst; indicating that hSec10 functions, directly or indirectly, in cellular processes far beyond its previously known role in directing vesicular traffic. These results suggest that there are previously unsuspected signaling or other pathways connecting membrane traffic, protein synthesis, and, especially, the vital, yet poorly understood process of morphogenesis of higher order epithelial structures, such as cysts and tubules. Understanding the mechanisms underlying these newly discovered connections will be the subject of further investigations. Moreover, we can speculate that components of this signaling pathway may be homologous to components that control cyst and tubule morphogenesis in *Drosophila* and *C. elegans*.

ACKNOWLEDGMENTS

We thank S. Chapin and F. Luton for their helpful discussion and reading of this manuscript. P. DeCamilli is acknowledged for help in cloning hSec10. S. Huling and the University of California, San Francisco, Liver Center are gratefully acknowledged for their assistance with electron microscopy. R. Bacallao and A. Wandinger-Ness are acknowledged for sending us their manuscript before publication. Finally, we thank W.J. Nelson, K. Grindstaff, and C. Yeaman for their helpful discussion and sharing of unpublished data before publication. This study was supported by National Institutes of Health and DAMD (DAMD-17-97-1-7249) grants to K.E.M, and National Institutes of Health, a National Kidney Foundation Young Investigator Award, and a Northern California National Kidney Foundation grant to J.H.L.

REFERENCES

Adams, A.E., Johnson, D.I., Longnecker, R.M., Sloat, B.F., and Pringle, J.R. (1990). CDC42 and CDC43, two additional genes involved in budding and the establishment of cell polarity in the yeast *Saccharomyces cerevisiae*. J. Cell Biol. *111*, 131–142.

Appel, D., Pilarsky, C., Graichen, R., and Koch-Brandt, C. (1996). Sorting of gp80 (GPIII, clusterin), a marker protein for constitutive apical secretion in Madin-Darby canine kidney (MDCK) cells, into the regulated pathway in the pheochromocytoma cell line PC12. Eur. J. Cell Biol. *70*, 142–149.

Arnould, T., Sellin, L., Benzing, T., Tsiokas, L., Cohen, H.T., Kim, E., and Walz, G. (1999). Cellular activation triggered by the autosomal dominant polycystic kidney disease gene product PKD2. Mol. Biol. Cell *19*, 3423–3434.

Avner, E.D., Sweeney, W.E., Jr., and Nelson, W.J. (1992). Abnormal sodium pump distribution during renal tubulogenesis in congenital murine polycystic kidney disease. Proc. Natl. Acad. Sci. USA *89*, 7447–7451.

Ayscough, K.R., Stryker, J., Pokala, N., Sanders, M., Crews, P., and Drubin, D.G. (1997). High rates of actin filament turnover in budding yeast and roles for actin in establishment and maintenance of cell polarity revealed using the actin inhibitor latrunculin-A. J. Cell Biol. *137*, 399–416.

Balda, M.S., and Matter, K. (2000). The tight junction protein ZO-1 and an interacting transcription factor regulate ErbB-2 expression. EMBO J. *19*, 2024–2033.

Balkovetz, D.F., and Lipschutz, J.H. (1998). Hepatocyte growth factor and the kidney: it's not just for the liver. Int. Rev. Cytol. *186*, 225–260.

Bao, Q., and Hughes, R.C. (1995). Galectin-3 expression and effect on cyst enlargement and tubulogenesis in kidney epithelial MDCK cells cultured in three-dimensional matrices *in vitro*. J. Cell Sci. *108*, 2791–2800.

Bao, Q., and Hughes, R.C. (1999). Galectin-3 and polarized growth within collagen gels of wild-type and ricin-resistant MDCK renal epithelial cells. Glycobiology *9*, 489–495.

Barros, E.J., Santos, O.F., Matsumoto, K., Nakamura, T., and Nigam, S.K. (1995). Differential tubulogenic and branching morphogenetic

activities of growth factors: implications for epithelial tissue development. Proc. Natl. Acad. Sci. USA *92*, 4412–4416.

Beitel, G.J., and Krasnow, M.A. (2000). Genetic control of epithelial tube size in the *Drosophila* tracheal system. Development *127*, 3271–3282.

Boccaccio, C., Ando, C., Tamagnone, L., Bardelli, A., Michieli, P., Battistini, C., and Comoglio, P.M. (1998). Induction of epithelial tubules by growth factor HGF depends on the STAT pathway. Nature *391*, 285–288.

Bredt, D.S. (2000). Reeling CASK into the nucleus. Nature *404*, 241–242.

Breitfeld, P., Casanova, J.E., Harris, J.M., Simister, N.E., and Mostov, K.E. (1989). Expression and analysis of the polymeric immunoglobulin receptor. Methods Cell Biol. *32*, 329–337.

Bretscher, M.S., and Aguado-Velasco, C. (1998). Membrane traffic during cell locomotion. Curr. Opin. Cell Biol. *10*, 537–541.

Brinkmann, V., Foroutan, H., Sachs, M., Weidner, K.M., and Birchmeier, W. (1995). Hepatocyte growth factor/scatter factor induces a variety of tissue-specific morphogenic programs in epithelial cells. J. Cell Biol. *131*, 1573–1586.

Buechner, M., Hall, D.H., Bhatt, H., and Hedgecock, E.M. (1999). Cystic canal mutants in *Caenorhabditis elegans* are defective in the apical membrane domain of the renal (excretory) cell. Dev. Biol. *214*, 227–241.

Butz, S., Okamoto, T., and Sudhoff, T.C. (1998). A tripartite protein complex with the potential to couple synaptic vesicle exocytosis to cell adhesion in brain. Cell *94*, 773–782.

Byers, B. (1981). Cytology of the yeast life cycle. In: Molecular Biology of the Yeast *Saccharomyces*: Life Cycle and Inheritance, eds. J.N. Strathern, E.W. Jones, and J.R. Broach), Cold Spring Harbor, NY: Cold Spring Harbor Laboratory, 59–96.

Cantley, L.G., Barros, E.J., Gandhi, M., Rauchman, M., and Nigam, S.K. (1994). Regulation of mitogenesis, motogenesis, and tubulogenesis by hepatocyte growth factor in renal collecting duct cells. Am. J. Physiol. *267*, F271–F280.

Charron, A.J., Nakamura, S., Bacallao, R., and Wandinger-Ness, A. (2000). Compromised cytoarchitecture and polarized trafficking in autosomal dominant polycystic kidney disease cells. J. Cell Biol. *149*, 111–124.

Consortium, T.I.P.D. (1995). Polycystic kidney disease: the complete structure of the PKD1 gene and its protein. Cell *81*, 289–298.

Crepaldi, T., Gautreau, A., Comoglio, P.M., Louvard, D., and Arpin, M. (1997). Ezrin is an effector of hepatocyte growth factor-mediated migration and morphogenesis in epithelial cells. J. Cell Biol. *138*, 423–434.

Daniel, J., and Reynolds, A.B. (1999). The catenin p120ctn interacts with Kaiso, a novel BTB/POZ domain zinc finger transcription factor. Mol. Biol. Cell *19*, 3614–3623.

Derman, M.P., Cunha, M.J., Barros, E.J., Nigam, S.K., and Cantley, L.G. (1995). HGF-mediated chemotaxis and tubulogenesis require activation of the phosphatidylinositol 3-kinase. Am. J. Physiol. *268*, F1211–F1217.

Doria, M., Salcini, A.E., Colombo, E., Parslow, T.G., Pelicci, P.G., and Di Fiore, P.P. (1999). The Eps15 homology (EH) domain-based interaction between Eps15 and Hrb connects the molecular machinery of endocytosis to that of nucleocytosolic transport. J. Cell Biol. *147*, 1379–1384.

Farkas, V., Kovarik, J., Kosinova, A., and Bauer, S. (1974). Autoradiographic study of mannan incorporation into the growing cell wall of *Saccharomyces cerevisiae*. J. Bacteriol. *117*, 265–269.

Field, C., and Schekman, R. (1980). Localized secretion of acid phosphatase reflects the pattern of cell surface growth in *Saccharomyces cerevisiae*. J. Cell Biol. *86*, 123–128.

Finger, F.P., Hughes, T.E., and Novick, P. (1998). Sec3p is a spatial landmark for polarized secretion in budding yeast. Cell *92*, 559–571.

Finger, F.P., and Novick, P. (1998). Spatial regulation of exocytosis: lessons from yeast. J. Cell Biol. *142*, 609–612.

Friedrich, G.A., Hildebrand, J.D., and Soriano, P. (1997). The secretory protein Sec8 is required for paraxial mesoderm formation in the mouse. Dev. Biol. *192*, 364–374.

Gabow, P.A. (1993). Autosomal dominant polycystic kidney disease. N. Engl. J. Med. *329*, 332–340.

Gherardi, E., Gray, J., Stoker, M., Perryman, M., and Furlong, R. (1989). Purification of scatter factor, a fibroblast-derived basic protein that modulates epithelial interactions and movement. Proc. Natl. Acad. Sci. USA *86*, 5844–5848.

Goode, B.L., Drubin, D.G., and Barnes, G. (2000). Functional cooperation between the microtubule and actin cytoskeleton. Curr. Opin. Cell Biol. *12*, 63–71.

Gottardi, C.J., Arpin, M., Fanning, A.S., and Louvard, D. (1996). The junction-associated protein, zonula occludens-1, localizes to the nucleus before the maturation and during the remodeling of cell-cell contacts. Proc. Natl. Acad. Sci. USA *93*, 10779–10784.

Grantham, J.J. (1997). Mechanisms of progression in autosomal dominant polycystic kidney disease. Kidney Int. *52*, S93–S97.

Grindstaff, K.K., Yeaman, C., Anandasabapathy, N., Hsu, S., Rodriguez-Boulan, R., Scheller, R.H., and Nelson, W.J. (1998). Sec6/8 complex is recruited to cell-cell contacts and specifies transport vesicle delivery to the basal-lateral membrane in epithelial cells. Cell *93*, 731–740.

Gumbiner, B.M. (1992). Epithelial morphogenesis [comment]. Cell *69*, 385–387.

Guo, W., Grant, A., and Novick, P. (1999a). Exo84p is an exocyst protein essential for secretion. J. Biol. Chem. *274*, 23558–23564.

Guo, W., Roth, D., Gatti, E., De Camilli, P., and Novick, P. (1997). Identification and characterization of homologues of the Exocyst component Sec10p. FEBS Lett. *404*, 135–139.

Guo, W., Roth, D., Walch-Solimena, C., and Novick, P. (1999b). The exocyst is an effector for Sec4p, targeting secretory vesicles to sites of exocytosis. EMBO J. *18*, 1071–1080.

Haddad, A., and Turkewitz, A.P. (1997). Analysis of exocytosis mutants indicates close coupling between regulated secretion and transcription activation in *Tetrahymena*. Proc. Natl. Acad. Sci. USA *94*, 10675–10680.

Haskins, J., Gu, L., Wittchen, E.S., Hibbard, J., and Stevenson, B.R. (1998). Zo-3, a novel member of the MAGUK protein family found at the tight junction, interacts with zo-1 and occludin. J. Cell Biol. *141*, 199–208.

Hsu, S., Hazuka, C.D., Roth, R., Foletti, D.L., Heuser, J., and Scheller, R.H. (1998). Subunit composition, protein interactions, and structures of the mammalian brain sec6/8 complex and septin filaments. Neuron *20*, 1111–1122.

Hsueh, Y., Wang, T., Yang, F., and Sheng, M. (2000). Nuclear translocation and transcription by the membrane-associated guanylate kinase CASK/LIN-2. Nature *404*, 298–302.

Korinek, V., Barker, N., Morin, P.J., Wichen, D.V., Weger, R.D., Kinzler, K.W., Vogelstein, B., and Clevers, H. (1997). Constitutive transcriptional activation by a β-catenin-Tcf complex in APC−/− colon carcinoma. Science *275*, 1784–1787.

Kretzschmar, M., and Massague, J. (1998). SMADS: mediators and regulators of TGF-beta signaling. Curr. Opin. Genet. Dev. *8*, 103–111.

Kroschewski, R., Hall, A., and Mellman, I. (1999). Cdc42 controls secretory and endocytic transport to the basolateral plasma membrane of MDCK cells. Nat. Cell Biol. *1*, 8–13.

Le Bivic, A., Sambuy, Y., Mostov, K., and Rodriguez-Boulan, E. (1990). Vectorial targeting of an endogenous apical membrane sialoglycoprotein and uvomorulin in MDCK cells. J. Cell Biol. *110*, 1533–1539.

Lecuit, T., and Wieschaus, E. (2000). Polarized insertion of new membrane from a cytoplasmic reservior during cleavage of the *Drosophila* embryo. J. Cell Biol. *150*, 849–860.

Leonard, W.J., and O'Shea, J.J. (1998). JAKS and STATS: biological implications. Annu. Rev. Immunol. *16*, 293–322.

Lewis, J.M., Baskaran, R., Taagepera, S., Schwarzt, M.A., and Wang, J.Y. (1996). Integrin regulation of c-Abl tyrosine kinase activity and cytoplasmic-nuclear transport. Proc. Natl. Acad. Sci. USA *93*, 15174–15179.

Li, D., and Mrsny, R.J. (2000). Oncogenic Raf-1 disrupts epithelial tight junctions via downregulation of occludin. J. Cell Biol. *148*, 791–800.

Lindstedt, R., Apodaca, G., Barondes, S.H., Mostov, K.E., and Leffler, H. (1993). Apical secretion of a cytosolic protein by Madin-Darby canine kidney cells. Evidence for polarized release of an endogenous lectin by a nonclassical secretory pathway. J. Biol. Chem. *268*, 11750–11757.

Lipschutz, J.H. (1998). The molecular development of the kidney: a review of the results of gene disruption studies. Am. J. Kidney Dis. *31*, 383–397.

Louvard, D. (1980). Apical membrane aminopeptidase appears at site of cell-cell contact in cultured kidney epithelial cells. Proc. Natl. Acad. Sci. USA *77*, 4132–4136.

Luton, F., Cardone, M.H., Zhang, M., and Mostov, K.E. (1998). Role of tyrosine phosphorylation in ligand-induced regulation of transcytosis of the polymeric Ig receptor. Mol. Biol. Cell *9*, 1787–1802.

Metzger, R.J., and Krasnow, M.A. (1999). Genetic control of branching morphogenesis. Science *284*, 1635–1639.

Mochizuki, T., Wu, G., Hayashi, T., Xenophontos, S.L., Veldhuisen, B., Saris, J.J., Reynolds, D.M., Cai, Y., Gabow, P.A., Pierides, A., Kimberling, W.J., Breuning, M.H., Deltas, C.C., Peters, D.J.M., and Somlo, S. (1996). *PKD2*, a gene for polycystic kidney disease that encodes an integral membrane protein. Science *272*, 1339–1342.

Montesano, R., Matsumoto, K., Nakamura, T., and Orci, L. (1991a). Identification of a fibroblast-derived epithelial morphogen as hepatocyte growth factor. Cell *67*, 901–908.

Montesano, R., Schaller, G., and Orci, L. (1991b). Induction of epithelial tubular morphogenesis in vitro by fibroblast-derived soluble factors. Cell *66*, 697–711.

Morin, P.J., Sparks, A.B., Korinek, V., Barker, N., Clevers, H., Vogelstein, B., and Kinzler, K.W. (1997). Activation of β-catenin-Tcf signaling in colon cancer by mutations in β-catenin or APC. Science *275*, 1787–1790.

Mostov, K.E., Verges, M., and Altschuler, Y. (2000). Membrane traffic in polarized epithelial cells. Curr. Opin. Cell Biol. *12*, 483–490.

Noren, N.K., Liu, B.P., Burridge, K., and Kreft, B. (2000). p120 catenin regulates the actin cytoskeleton via Rho family GTPases. J. Cell Biol. *150*, 567–579.

Novick, P., Field, C., and Schekman, R. (1980). Identification of 23 complementation groups required for post-translational events in the yeast secretory pathway. Cell *21*, 205–221.

Orzech, E., Cohen, S., Weiss, A., and Aroeti, B. (2000). Interactions between the exocytic and endocytic pathways in polarized Madin Darby canine kidney cells. J. Biol. Chem. *275*, 15207–15219.

Peifer, M. (1997). β-Catenin as oncogene: the smoking gun. Science *275*, 1752–1753.

Pollack, A.L., Barth, A.I.M., Altschuler, Y., Nelson, W.J., and Mostov, K.E. (1997). Dynamics of β-catenin interactions with APC protein regulate epithelial tubulogenesis. J. Cell Biol. *137*, 1651–1662.

Pollack, A.L., Runyan, R.B., and Mostov, K.E. (1998). Morphogenetic mechanisms of epithelial tubulogenesis: MDCK cell polarity is transiently rearranged without loss of cell-cell contact during scatter factor/hepatocyte growth factor-induced tubulogenesis. Dev. Biol. *204*, 64–79.

Roth, D., Guo, W., and Novick, P. (1998). Dominant negative alleles of SEC10 reveal distinct domains involved in secretion, and morphogenesis in yeast. Mol. Biol. Cell *9*, 1725–1739.

Rubinfeld, B., Robbins, P., El-Gamil, M., Albert, I., Porfiri, E., and Polakis, P. (1997). Stabilization of β-catenin by genetic defects in melanoma cell lines. Science *275*, 1790–1792.

Sakurai, H., Barros, E.J., Tsukamoto, T., Barasch, J., and Nigam, S.K. (1997a). An in vitro tubulogenesis system using cell lines derived from the embryonic kidney shows dependence on multiple soluble growth factors. Proc. Natl. Acad. Sci. USA *94*, 6279–6284.

Sakurai, H., Tsukamoto, T., Kjelsberg, C.A., Cantley, L.G., and Nigam, S.K. (1997b). EGF receptor ligands are a large fraction of in vitro branching morphogens secreted by embryonic kidney. Am. J. Physiol. *273*, F463–F472.

Sambrook, J., Fritsch, E.F., and Maniatis, T. (1989). Expression of cloned genes in cultured mammalian cells. In: Molecular Cloning: A Laboratory Manual, eds. J. Sambrook, E.F. Fritsch, and T. Maniatis), Cold Spring Harbor, New York: Cold Spring Harbor Laboratory Press, 16.30–16.36.

Santos, O.F., Moura, L.A., Rosen, E.M., and Nigam, S.K. (1993). Modulation of HGF-induced tubulogenesis and branching by multiple phosphorylation mechanisms. Dev. Biol. *159*, 535–548.

Santos, O.F., and Nigam, S.K. (1993). HGF-induced tubulogenesis and branching of epithelial cells is modulated by extracellular matrix and TGF-beta. Dev. Biol. *160*, 293–302.

Sato, S., Burdett, I., and Hughes, R.C. (1993). Secretion of the baby hamster kidney 30-kDa galactose-binding lectin from polarized and nonpolarized cells: a pathway independent of the endoplasmic reticulum-Golgi complex. Exp. Cell Res. *207*, 8–18.

Saxen, L. (1987). Organogenesis of the Kidney. Cambridge: Cambridge University Press.

Simons, K., and Fuller, S.D. (1985). Cell surface polarity in epithelia. Annu. Rev. Cell Biol. *1*, 295–340.

Stoker, M., Gherardi, E., Perryman, M., and Gray, J. (1987). Scatter factor is a fibroblast-derived modulator of epithelial cell mobility. Nature *327*, 239–242.

Stoker, M., and Perryman, M. (1985). An epithelial scatter factor released by embryo fibroblasts. J. Cell Sci. *77*, 209–223.

Terbush, D.R., Maurice, T., Roth, D., and Novick, P. (1996). The exocyst is a multiprotein complex required for exocytosis in *Saccharomyces cerevisiae*. EMBO J. *15*, 6483–6494.

Thiery, G., Bernier, J., and Bergeron, M. (1995). A simple technique for staining of cell membranes with imidazole and osmium tetroxide. J. Histocytochem. *43*, 1079–1084.

Thiery, J.P., and Boyer, B. (1992). The junction between cytokines and cell adhesion. Curr. Opin. Cell Biol. *4*, 782–792.

Ting, A.E., Hazuka, C.D., Hsu, S.C., Kirk, M.D., Bean, A.J., and Scheller, R.H. (1995). rSec6 and rSec8, mammalian homologs of

yeast proteins essential for secretion. Proc. Natl. Acad. Sci. USA *92*, 9613–9617.

Tkacz, J.S., and Lampen, J.O. (1972). Wall replication in *Saccharomyces* species: use of fluorescein-conjugated concanavalin A to reveal the site of mannan insertion. J. Gen. Microbiol. *72*, 243–247.

Urban, J., Parczyk, K., Leutz, A., Kayne, M., and Kondor-Koch, C. (1987). Constitutive apical secretion of an 80-kd sulfated glycoprotein complex in the polarized epithelial Madin Darby canine kidney cell line. J. Cell Biol. *105*, 2735–2743.

Vainio, S., and Muller, U. (1997). Inductive tissue interactions, cell signaling, and the control of kidney organogenesis. Cell *90*, 975–978.

Weidner, K.M., Sachs, M., Riethmacher, D., and Birchmeier, W. (1995). Mutation of juxtamembrane tyrosine residue 1001 suppresses loss-of-function mutations of the met receptor in epithelial cells. Proc. Natl. Acad. Sci. USA *92*, 2597–2601.

Wilson, P.D., Sherwood, A.C., Palla, K., Du, J., Watson, R., and Norman, J.T. (1991). Reversed polarity of Na+-K+-ATPase: mislocalization to apical plasma membranes in polycystic kidney disease epithelia. Am. J. Physiol. *260*, F420–F430.

Yeaman, C., Grindstaff, K.K., and Nelson, W.J. (1999). New perspectives on mechanisms involved in generating cell polarity. Physiol. Rev. *79*, 73–98.